Table S1 Selected polymers for initial TGA analysis.

Designation	Polymer	Structure of polymer
PS	Polystyrene	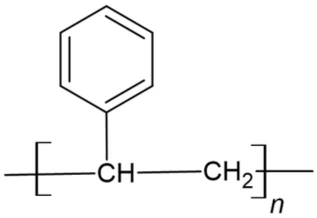
COC	Copolymer ethylene norbornene	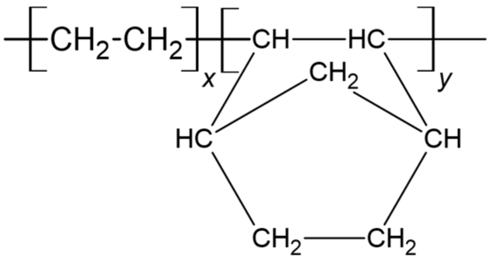
PEEK	Polyetheretherketone	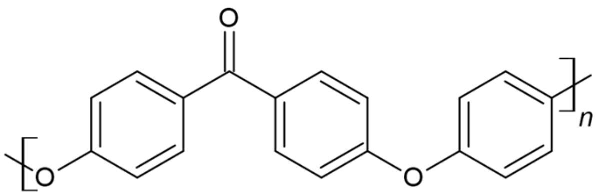
PC	Polycarbonate	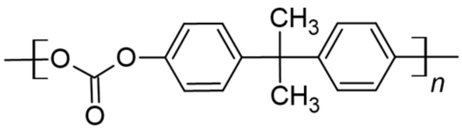

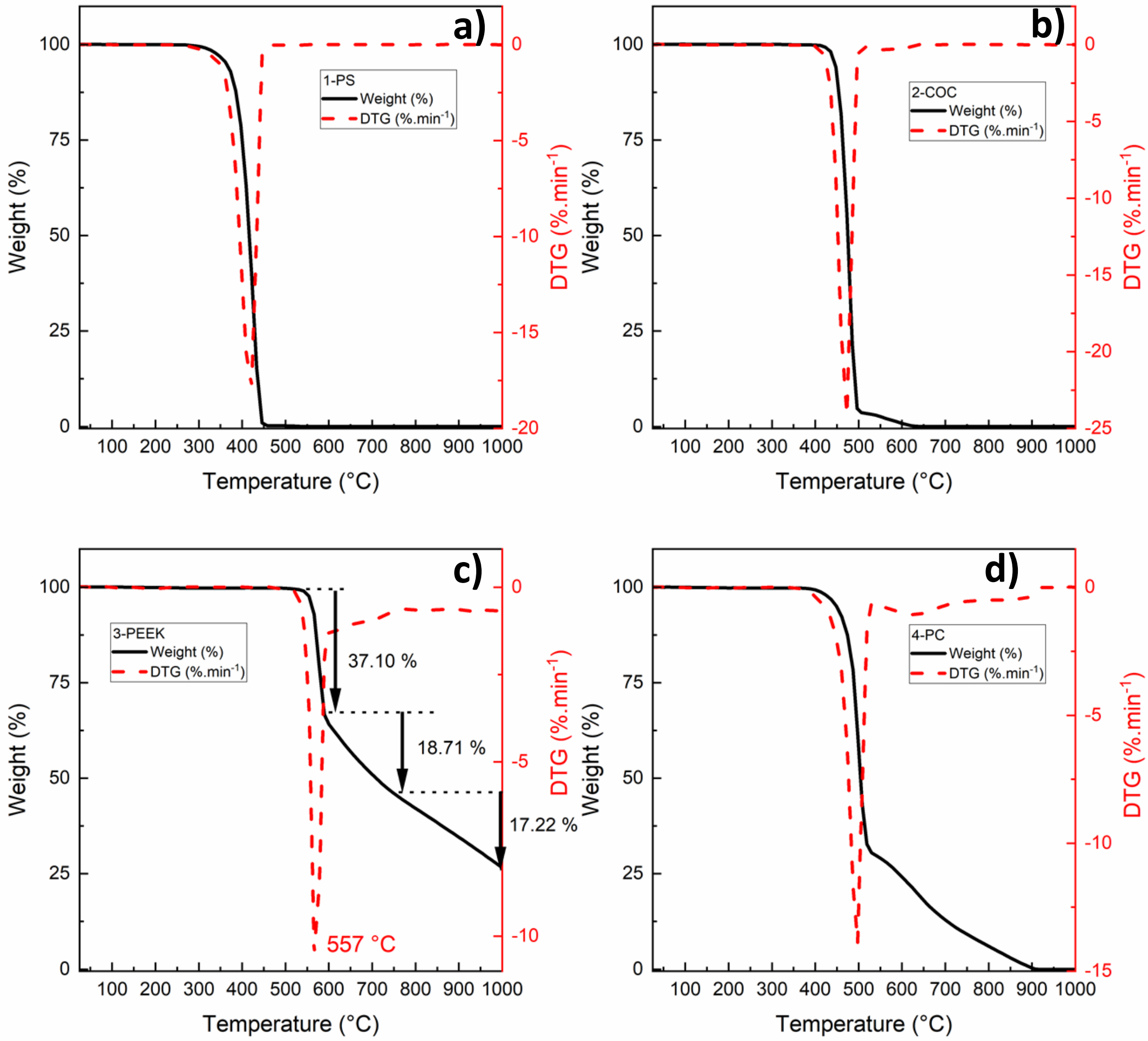

Fig.S1 Initial TGA of selected polymers.

Table S2 Chemical composition of pristine PEEK and pyrolyzed PEEK determined by XRF.

	Material	
	Pristine PEEK	Pyrolyzed PEEK
Element	wt%	wt%
Mg	< 0.0020	< 0.0028
Al	< 0.0020	0.077
Si	0.059	0.377
P	0.154	0.519
S	0.021	0.028
Cl	0.038	0.001
K	0.004	0.324
Ca	0.103	0.285
Ti	0.001	0.007
V	0.0000	0.000
Cr	0.000	0.003
Mn	0.000	0.003
Fe	0.003	0.060

Co	< 0.0004	0.001
Ni	0.001	0.003
Cu	0.000	0.000
Zn	0.000	0.004
Ga	0.000	0.000
Ge	0.0000	0.0000
As	0.0000	0.000
Se	0.0000	0.0000
Br	0.0000	0.000
Rb	0.000	0.000
Sr	0.000	0.000
Y	0.000	0.000
Zr	< 0.0001	0.000
Nb	0.000	0.000
Mo	0.001	0.001
Ag	< 0.0002	< 0.0002
Cd	0.000	0.000
Sn	< 0.0003	0.000
Sb	< 0.0003	< 0.0003
Te	0.000	0.000
I	< 0.0003	0.000
Cs	< 0.0004	< 0.0003
Ba	< 0.0002	< 0.0002
La	0.003	0.000
Ce	< 0.0002	< 0.0002
Pr	< 0.0002	< 0.0001
Nd	0.000	0.001
Hf	0.000	0.000
Ta	0.002	0.002
W	0.001	0.003
Hg	< 0.0001	< 0.0001
Tl	0.0000	0.000
Pb	0.000	0.000
Bi	< 0.0001	< 0.0001
Th	0.000	0.000
U	0.000	< 0.0001
Summary:	0.40	1.70

Table S3 FTIR bands

Wavenumbers (cm^{-1})	**Assignment of band**	**Note**
3309	stretching vibration of O-H in alcohol and phenols	
3180	stretching vibration of O-H in moisture	
3047	stretching vibration of =C-H in aromatic hydrocarbons	
2956	stretching vibration of C-H in aliphatic hydrocarbons (alkanes); vibration of CH_3 groups	asymmetrical mode
2874		symmetrical mode
2922	stretching vibration of C-H in aliphatic hydrocarbons (alkanes);	asymmetrical mode

2852	vibration of CH_2 groups	symmetrical mode
1709	stretching vibration of C=O in esters	
1585	stretching vibration of C=C in aromatic hydrocarbons	skeletal ring breathing mode
1405	deformation vibration of C-H in aliphatic hydrocarbons	CH_2 groups
1332		CH groups
1308		CH_2 groups
1173	stretching vibration of C-O in esters	
1030	stretching vibration of C-O in esters	
1252	stretching vibration of C-OH in phenols	
1118	stretching vibration of C-OH in aliphatic alcohols	secondary alcohols
1061		primary alcohols
866	out-of-plane deformation of =C-H in aromatic hydrocarbons	1 isolated H atom
806		2 adjacent H atoms
793		3 adjacent H atoms
744		4 or 5 adjacent H atoms

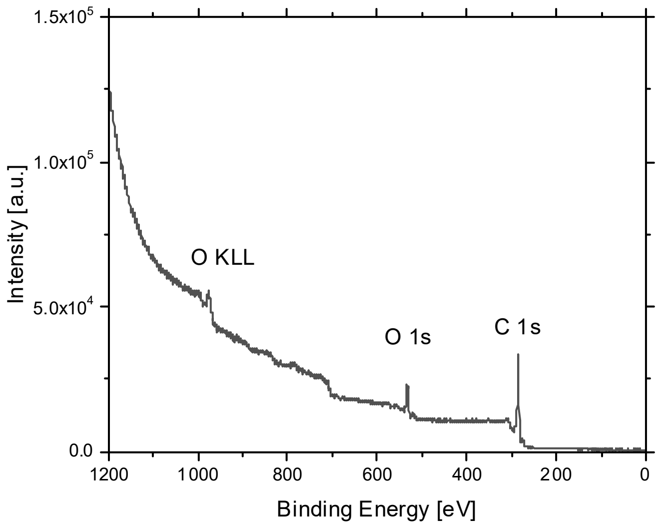

Fig.S2 The survey XPS spectra of pyrolyzed PEEK sample.

Table S4 Parameters of the models applied to kinetic test data.

Model	**Parameter**	**Pharmaceutical**	
		Diclofenac	**Ofloxacine**
Pseudo-first order	q_e *(mg g⁻¹)*	0.18	0.16
	K_1 *(min⁻¹)*	0.41	0.22
	R^2_{adj}	0.99	0.98
	X^2	$1.85 \cdot 10^{-5}$	$7.57 \cdot 10^{-5}$
Pseudo-second order	q_e *(mg g⁻¹)*	0.20	0.19

	K_2 *(g mg^{-1} min^{-1})*	2.45	1.18
	R^2_{adj}	0.99	0.98
	X^2	$2.12 \cdot 10^{-5}$	$5.83 \cdot 10^{-5}$
Elovich equation	*a (mg g^{-1} min^{-1})*	0.18	0.07
	b (mg g^{-1})	22.34	19.90
	R^2_{adj}	0.97	0.98
	X^2	$1.25 \cdot 10^{-4}$	$7.61 \cdot 10^{-5}$
Intraparticle diffusion	k_{Diff1} *(mg g^{-1} min$^{0.5}$)*	0.01	0.01
	C_1 *(mg g^{-1})*	-0.01	-0.00
	R_1^2	0.99	0.98
	k_{Diff2} *(mg g^{-1} min$^{0.5}$)*	0.00	0.00
	C_2 *(mg g^{-1})*	0.10	0.06
	R_2^2	0.97	0.99
	k_{Diff3} *(mg g^{-1} min$^{0.5}$)*	$6.67 \cdot 10^{-4}$	0.00
	C_3 *(mg g^{-1})*	0.16	0.05
	R_3^2	0.97	0.99

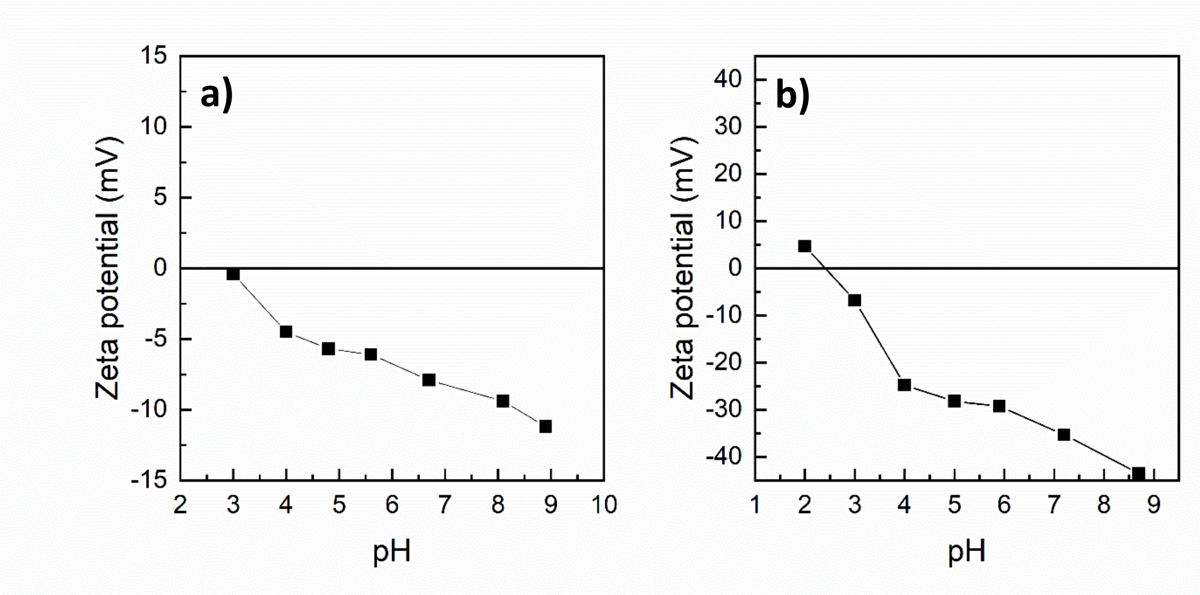

Fig.S3 Isoelectric point of a pyrolyzed PEEK a) in KCl solution, b) in distilled water.

Table S5 Zeta potential

Material	Solution	Concentration (mg L^{-1})	Zeta potential (mV)	St.deviation
pyrolyzed PEEK	water	-	-28.1	±0.7
pyrolyzed PEEK	KCl	74.55	-8.8	±3.5
pyrolyzed PEEK	Ofloxacine	168.7×10^{-3}	-28.4	±0.3
pyrolyzed PEEK	Diclofenac	148.7×10^{-3}	-27.3	±0.7

Table S6 Parameters of the models applied to equilibrium test data.

Model	**Parameter**	**Pharmaceutical**	
		Diclofenac	**Ofloxacine**

Langmuir	Q_{max} (mg g^{-1})	2.05	2.79
	K_L (L g^{-1})	5.83	0.13
	R^2_{adj}	0.90	0.91
	X^2	0.02	0.11
Freundlich	K_F (mg g^{-1})/(mg L^{-1})^n	1.47	0.90
	n	0.13	0.29
	R^2_{adj}	0.91	0.99
	X^2	0.02	0.02
Redlich-Peterson	*KRP*	21.62	201.61
	aRP	12.58	214.15
	g	0.93	0.73
	R^2_{adj}	0.99	0.98
	X^2	0.00	0.02
Dubinin-Radushkevich	q_{DR}(mg g^{-1})	1.98	2.15
	K_{DR} (mol^2 kJ^{-2})	0.03	0.04
	E (kJ mol^{-1})	0.50	0.48
	R^2_{adj}	0.84	0.79
	X^2	0.04	0.25

Table S7 Kinetic parameters of diclofenac adsorption reported in literature.

Publication	Year	Material	c_0 (mg L^{-1})	Model
this work		pyrolyzed PEEK based carbonaceous sorbent	0.1485	pseudo-first order
Viotti et al. [9]	2019	moringa oleifera pod	50	pseudo-second order
		activated carbon	50	pseudo-second order
Avcu et al. [10]	2021	sycamore ball activated carbon	10–50	pseudo-second order
Bouhcain et al. [11]	2022	argan fruit shells activated carbon	100	pseudo-second order
Bernardo et al. [12]	2016	potato peel waste activated carbon	50	
Oumabady et al. [13]	2022	sludge derived hydrochar	10–50	pseudo-second order
de Luna et al. [14]	2017	cocoa pod husk biosorbent		pseudo-second order
Lonappan et al. [15]	2018	pig manure biochar	2	pseudo-second order
		pine wood biochar	2	pseudo-second order

Table S8 Kinetic parameters of ofloxacin adsorption reported in literature.

Publication	Year	Material	c_0 (mg L^{-1})	Model

this work		pyrolyzed PEEK based carbonaceous sorbent	0.1687	pseudo-second order
Kong et al. [16]	2017	luffa sponge activated carbon	30–70	pseudo-second order
Weng et al. [17]	2021	calcined magnetic iron nanoparticles	5–50	pseudo-second order
Liu et al. [18]	2022	natural ilmenite-biochar composite	2–25	pseudo-second order
He et al. [19]	2022	N-doped activated carbon	110–250	pseudo-second order
Akhtar et al. [20]	2021	various organic waste based biochars		pseudo-second order
		municipal organic waste based biochar pyrolyzed at 300 °C		Elovich
Sulaiman et al. [21]	2022	chemically modified cassava stem activated carbon		pseudo-second order
Wang et al. [22]	2022	copper-doped ZIF-8	260	pseudo-second order
Zhang et al. [23]	2011	modified coal fly ash	100	pseudo-second order
Zhu et al. [24]	2018	chitosan/biochar composite	10	pseudo-second order

Table S9 Adsorption capacities of diclofenac reported in literature.

Publication	Year	Material	q_{max} (mg g^{-1})
this work		pyrolyzed PEEK based carbonaceous sorbent	2.25
de Franco et al. [25]	2018	activated carbon	36.23
Viotti et al. [9]	2019	moringa oleifera pod	56.692
		activated carbon	47.125
Avcu et al. [10]	2021	sycamore ball activated carbon	178.89
Bouhcain et al. [11]	2022	argan fruit shells activated carbon	126.16
Bernardo et al. [12]	2016	potato peel waste activated carbon	68.5
Oumabady et al. [13]	2022	sludge derived hydrochar	31.746
Jodeh et al. [26]	2016	cyclamen persicum tubers activated carbon	22.22
Lonappan et al. [15]	2018	pig manure biochar	12.5
		pine wood biochar	0.526
de Luna et al. [14]	2017	cocoa pod husk biosorbent	0.474

Table S10 Adsorption capacities of ofloxacin reported in literature.

Publication	Year	Material	q_{max} (mg g^{-1})
this work		pyrolyzed PEEK based carbonaceous sorbent	2.84
Kong et al. [16]	2017	luffa sponge activated carbon	131.93
Weng et al. [17]	2021	calcined magnetic iron nanoparticles	17.5
Liu et al. [18]	2022	natural ilmenite-biochar composite	14.226
He et al. [19]	2022	N-doped activated carbon	796.153
Akhtar et al. [20]	2021	various organic waste based biochars	234.3–3 702
Wang et al. [22]	2022	copper-doped ZIF-8	757.58
Zhang et al. [23]	2011	modified coal fly ash	2.41
Zhu et al. [24]	2018	chitosan/biochar composite	6.64

References (Supporting information)

[1] LAGERGREN, S. About the theory of so-called adsorption of soluble substances. Kungliga Svenska Vetenskapsakademiens Handlingar, 1898, 24(4), 1-39.
[2] BLANCHARD, G., M. MAUNAYE AND G. MARTIN REMOVAL OF HEAVY-METALS FROM WATERS BY MEANS OF NATURAL ZEOLITES. Water Research, 1984, 18(12), 1501-1507.

[3] S. ROGINSKY, Y. B. Z. The catalytic oxidation of carbon monoxide on manganese dioxide. Acta Physicochimica URSS 1934, 1, 554.
[4] WEBER, W. J., MORRIS, J.C. Kinetics of adsorption of carbon from solution. Journal of the Sanitary Engineering Division, 1963, 89(2), 31-60.
[5] LANGMUIR, I. The adsorption of gases on plane surfaces of glass, mica and platinum. Journal of the American Chemical Society, 1918, 40(9), 1361-1403.
[6] FREUNDLICH, H. Über die Adsorption in Lösungen. Zeitschrift für Physikalische Chemie, 1906, 57, 385-471.
[7] REDLICH, O. AND D. L. PETERSON A USEFUL ADSORPTION ISOTHERM. Journal of Physical Chemistry, 1959, 63(6), 1024-1024.
[8] DUBININ, M., RADUSHKEVICH, L. Equation of the characteristic curve of activated charcoal. Chemisches Zentralblatt, 1947, 1(1), 875.
[9] VIOTTI, P. V., W. M. MOREIRA, O. A. A. DOS SANTOS, R. BERGAMASCO, et al. Diclofenac removal from water by adsorption on Moringa oleifera pods and activated carbon: Mechanism, kinetic and equilibrium study. Journal of Cleaner Production, May 2019, 219, 809-817.
[10] AVCU, T., O. UNER AND U. GECGEL Adsorptive removal of diclofenac sodium from aqueous solution onto sycamore ball activated carbon - isotherms, kinetics, and thermodynamic study. Surfaces and Interfaces, Jun 2021, 24.
[11] BOUHCAIN, B., D. CARRILLO-PENA, F. EL MANSOURI, Y. E. ZOUBI, et al. Removal of Emerging Contaminants as Diclofenac and Caffeine Using Activated Carbon Obtained from Argan Fruit Shells. Applied Sciences-Basel, Mar 2022, 12(6).
[12] BERNARDO, M., S. RODRIGUES, N. LAPA, I. MATOS, et al. High efficacy on diclofenac removal by activated carbon produced from potato peel waste. International Journal of Environmental Science and Technology, Aug 2016, 13(8), 1989-2000.
[13] OUMABADY, S., P. S. SELVARAJ, K. PERIASAMY, D. VEERASWAMY, et al. Kinetic and isotherm insights of Diclofenac removal by sludge derived hydrochar. Scientific Reports, Feb 2022, 12(1).
[14] DE LUNA, M. D. G., MURNIATI, W. BUDIANTA, K. K. P. RIVERA, et al. Removal of sodium diclofenac from aqueous solution by adsorbents derived from cocoa pod husks. Journal of Environmental Chemical Engineering, Apr 2017, 5(2), 1465-1474.
[15] LONAPPAN, L., T. ROUISSI, S. K. BRAR, M. VERMA, et al. An insight into the adsorption of diclofenac on different biochars: Mechanisms, surface chemistry, and thermodynamics. Bioresource Technology, Feb 2018, 249, 386-394.
[16] KONG, Q., X. HE, L. SHU AND M. S. MIAO Ofloxacin adsorption by activated carbon derived from luffa sponge: Kinetic, isotherm, and thermodynamic analyses. Process Safety and Environmental Protection, Nov 2017, 112, 254-264.
[17] WENG, X. L., W. L. CAI, G. OWENS AND Z. L. CHEN Magnetic iron nanoparticles calcined from biosynthesis for fluoroquinolone antibiotic removal from wastewater. Journal of Cleaner Production, Oct 2021, 319.
[18] LIU, Y. J., Y. YI, Z. W. WANG, W. YUAN, et al. Removal of ofloxacin from water by natural ilmenite-biochar composite: A study on the synergistic adsorption mechanism of multiple effects. Bioresource Technology, Nov 2022, 363.
[19] HE, S., Q. L. CHEN, G. Y. CHEN, G. B. SHI, et al. N-doped activated carbon for high-efficiency ofloxacin adsorption. Microporous and Mesoporous Materials, Apr 2022, 335.
[20] AKHTAR, L., M. AHMAD, S. IQBAL, A. A. ABDELHAFEZ, et al. Biochars' adsorption performance towards moxifloxacin and ofloxacin in aqueous solution: Role of pyrolysis temperature and biomass type. Environmental Technology & Innovation, Nov 2021, 24.
[21] SULAIMAN, N. S., M. H. M. AMINI, M. DANISH, O. SULAIMAN, et al. Characterization and Ofloxacin Adsorption Studies of Chemically Modified Activated Carbon from Cassava Stem. Materials, Aug 2022, 15(15).
[22] WANG, X. W., Y. J. ZHAO, Y. Q. SUN AND D. H. LIU Highly Effective Removal of Ofloxacin from Water with Copper-Doped ZIF-8. Molecules, Jul 2022, 27(13).

[23] ZHANG, C. L., F. ZHAO AND Y. WANG Thermodynamic and Kinetic Parameters of Ofloxacin Adsorption from Aqueous Solution onto Modified Coal Fly Ash. Russian Journal of Physical Chemistry A, Apr 2012, 86(4), 653-657.
[24] ZHU, C. M., Y. H. LANG, B. LIU AND H. X. ZHAO Ofloxacin Adsorption on Chitosan/Biochar Composite: Kinetics, Isotherms, and Effects of Solution Chemistry. Polycyclic Aromatic Compounds, May 2019, 39(3), 287-297.
[25] DE FRANCO, M. A. E., C. B. DE CARVALHO, M. M. BONETTO, R. D. SOARES, et al. Diclofenac removal from water by adsorption using activated carbon in batch mode and fixed-bed column: Isotherms, thermodynamic study and breakthrough curves modeling. Journal of Cleaner Production, Apr 2018, 181, 145-154.
[26] JODEH, S., ABDELWAHAB, F., JARADAT, N., WARAD, I., JODEH, W. Adsorption of diclofenac from aqueous solution using Cyclamen persicum tubers based activated carbon (CTAC). Journal of the Association of Arab Universities for Basic and Applied Sciences, 2016, 20, 32-38.